frontiers | Frontiers in Environmental Science

ORIGINAL RESEARCH
published: 12 July 2022
doi: 10.3389/fenvs.2022.860011

Optimization of the Electrocoagulation Process with Aluminum Electrodes for Rainwater Treatment

Alejandra Morales-Figueroa[1†], Elia Alejandra Teutli-Sequeira[2], Ivonne Linares-Hernández[3†], Verónica Martínez-Miranda[3†], Marco A. García-Morales[1] and Gabriela Roa-Morales[1]**

[1]Centro Conjunto de Investigación en Química Sustentable CCIQS, UAEM-UNAM Universidad Autónoma del Estado de México, Toluca, Mexico, [2]Cátedras CONACYT-IITCA, Toluca, Mexico, [3]Instituto Interamericano de Tecnología y Ciencias de Agua (IITCA), Universidad Autónoma del Estado de México, Toluca, Mexico

OPEN ACCESS

Edited by:
Hugo Olvera-Vargas,
Universidad Nacional Autonoma de Mexico, Mexico

Reviewed by:
Milad Mousazadeh,
Qazvin University of Medical Sciences, Iran
Orlando Garcia,
National University of Singapore, Singapore

***Correspondence:**
Elia Alejandra Teutli-Sequeira
aleteutlis@gmail.com
Gabriela Roa-Morales
groam@uaemex.mx

[†]These authors have contributed equally to this work

Specialty section:
This article was submitted to Water and Wastewater Management, a section of the journal Frontiers in Environmental Science

Received: 22 January 2022
Accepted: 17 June 2022
Published: 12 July 2022

Citation:
Morales-Figueroa A, Teutli-Sequeira EA, Linares-Hernández I, Martínez-Miranda V, García-Morales MA and Roa-Morales G (2022) Optimization of the Electrocoagulation Process with Aluminum Electrodes for Rainwater Treatment. Front. Environ. Sci. 10:860011. doi: 10.3389/fenvs.2022.860011

Rainwater collected in the Toluca region of Mexico with a pH of 6.25 was treated with an electrochemical process, and the efficiency of two supporting electrolytes were compared, one food grade (sea salt) and the other reagent grade (sodium sulfate). In the first stage, rainwater was characterized to detect the COD content, turbidity, metals such as zinc, iron, aluminum, and lead. Electrocoagulation treatment was performed with an electrochemical cell using aluminum electrodes to study the effect on COD and turbidity, as well as the removal of heavy metals present. The results obtained with response surface methodology and a central composite design reveal that the optimal conditions of the electrocoagulation treatment were a current density of 3.26 mA/cm^2 and a time of 11.38 min. Using sodium sulfate, the percentage of turbidity removal is 99.27% and COD 70.83%. The use of sea salt as a support electrolyte in these conditions allowed the removal of COD at 100%, turbidity at 100%, and Al 100%, Mn 84.29%, Zn 97.97%, Pb 46%, Fe 21%. Energy costs that are low lead to proven savings when using this system, indicating that this treatment is an option to both improve rainwater conditions and be able to make use of it safely.

Keywords: rainwater, electrocoagulation, aluminum electrodes, sea salt, support electrolyte effect, response surface

INTRODUCTION

Water sources are increasingly limited around the world due to increasing populations, climate change and contamination (Ding et al., 2017). An alternative water supply for drinking and non-drinking uses is rainwater (Teixeira & Ghisi, 2019). Rainwater has been used as drinking water for centuries, mainly in rural areas, and is accepted as an essential water resource. Additionally, it is a natural resource that can be simply collected and consumed in a variety of domestic, commercial and industrial applications, as well as for potable purposes (Ding et al., 2017). However, the quality of rainwater is susceptible to contamination by microorganisms, bird feces, urban pollution particles, dust from the wind, dust, pesticides, and dissolved organic gasses (SO_x, CO_2 and NO_x). It has a low pH (in the range of 4 78–5.85), whilst dissolved CO_2 (Omar et al., 2017; Khayan et al., 2019), polycyclic aromatic hydrocarbons, nutrients, heavy metals and salt have been identified as key pollutants, among others.

Zhang et al. (2014), summarized that stormwater was likely to contain: 1–36,200 mg/L of sediment, 5.80–112.2 μg/L of Pb, 0.1–6.94 mg/L of TP, and 507–16,000 MPN of *Escherichia coli* per 100 ml. Other

pathogens include parasites like *Giardia lamblia*, *Cryptosporidium parvum* and *Toxoplasma gondii*. Other bacteria like *Campylobacter*, *Salmonella*, *Leptospira*; *Pseudomonas*, *Klebsiella*, *Campylobacter* and *Staphylococcus* spp. *Areerachakul* (Kim et al., 2016; Ding et al., 2017; Jaiyeola, 2017; Leong et al., 2017; Waso et al., 2020) would also likely be found.

Rainwater should not be used without treatment due to the harmful health risks involved. The selected treatment train should be fit-for-purpose or tailored to the end-use. In an urban environment, rainwater is an alternative water resource that can be collected, treated, and distributed through decentralized rainwater harvesting and recycling systems. Traditional systems for treating contaminated water include: physical treatments, membranes, sand filtration, ultrafiltration (UF), reverse osmosis, UV radiation, pasteurization and chemical treatments such as chlorination, ozonation, and colloidal silver. In addition, oxidation, coagulation-flocculation and electrocoagulation (Ding et al., 2018; Waso et al., 2020) have also been used for greywater and black water. The difference between the two is that black water has fecal matter. Fecal matter is a haven for harmful bacteria and disease-causing pathogens. However, these techniques could be useful when the rainwater contains high levels of COD and BOD (Leong et al., 2017; Taffere et al., 2017; Teixeira and Ghisi, 2019).

The electrocoagulation process consists of an electrolysis cell that uses a pair of electrodes: the sacrificial anode (Al or Fe) is where the metal ions are electrogenerated by the oxidation reaction, which will form the coagulating species in solution with the products of the reduction reaction that occurs at the cathode, in which water is reduced to produce hydrogen and OH^-. The metallic ions react with the hydroxides, generating flocs where the contaminants are adsorbed in colloidal form. The lighter flocs separate with the help of the hydrogen bubbles at the cell surface, and when the flocs increase in size, they then generate the coagulation process and precipitate (Devlin et al., 2019; Xu et al., 2021).

Therefore, the advantages of electrocoagulation are that the cell is easy to operate, the removal of suspended solids is carried out by flotation and precipitation, it is feasible to control the amount of sludge and the energy used in the process can be supplied using a solar panel. (Dura and Breslin, 2019).

Due to the benefits provided by electrocoagulation, it has been widely used to eliminate various contaminants, such as organic matter, dyes, aromatic compounds, drugs and petroleum derivatives, among others, as well as inorganic matter such as metal ions in wastewater. (Taeyeon Verma, 2017; Kim et al., 2020; Padmaja et al., 2020; Xu et al., 2021).

The proper functioning of the electrocoagulation cell must consider several factors that affect the process, such as the current density applied, distance between the electrodes, electrode contact area, cell potential, mass transfer, pH, type of support electrolyte, concentration, and treatment time, among others. It has been verified that some parameters must be studied and selected according to the characteristics of the water to be treated (Izquierdo et al., 2010). The support electrolyte is one of the most relevant factors because if there is not enough ionic conductivity in the water to be treated, it is probable that the expected electrochemical reactions will not take place, because there will be a great resistance to the passage of the applied current (Yildiz et al., 2008; Maitlo et al., 2018). It is also recommended that the support electrolyte have strong characteristics, that is, that it completely dissociates, which is why NaCl, $NaHCO_3$, Na_2SO_4, NH_4Cl, and $NaNO_3$ have been recommended (Keyikoglu et al., 2019). The concentration and chemical nature of the supporting electrolyte are important since, in the case of using NaCl, the Cl- ions are capable of oxidizing at the anode, generating Cl_2, which acts as a disinfectant. However, it is possible that some chlorinated organic compounds may be generated that can increase the toxicity of the treated water. Another good alternative to be used as a supporting electrolyte is sea salt, which mainly contains Na, Cl, Mg, S, Ca, Br, and K (Adachi and Buseck, 2015).

In this work, it is proposed that rainwater be treated by electrocoagulation in order to explore the feasibility of applying this technology in places with scarce water resources where when it rains, water can be collected, treated and stored. With this, society would benefit from water of adequate quality, in addition to a great environmental impact due to the fact that the generation of sludge would be low and the energy could be supplied with a solar panel.

Consequently, the aim of this research was to evaluate the treatment of rainwater through an electrocoagulation process with Al electrodes for the removal of COD and turbidity. The operating parameters (current density, supporting electrolyte and time) were obtained using response surface methodology through a central composite model. It is well known that the supporting electrolyte is a parameter of great importance and that proper functioning of a cell depends on the ionic conductivity. For this reason, in this study, it is of great importance to verify the effect of two types of electrolytes using the minimum amount necessary. This is in order to establish whether the treated water is suitable for human consumption.

An optimization method is response surface methodology (RSM) obtained from statistical and mathematical methods that can be used to study the effect of diverse factors at several levels and their interactions. This method involves four main steps, which are: experiment design, model fitting, model verification, and determination of optimal conditions. Central Composite Design (CCD) is one of the most widely used techniques for RSM due to the need for fewer experiments (Darvishmotevalli et al., 2019).

MATERIALS AND METHODS

Rainwater Sample Collection and Sampling Site

The samples were collected in the open air in a 20 L high-density polypropylene container and kept under controlled conditions. Rainwater samples were collected during different rainy days in a rural area, located at coordinates 19–40′04.93′N and 99’.71‴56.69′E in Toluca, State of Mexico, Mexico. The rainwater collection was carried out during the rainy season of 2019, from May to September. Point A in **Figure 1** corresponds to

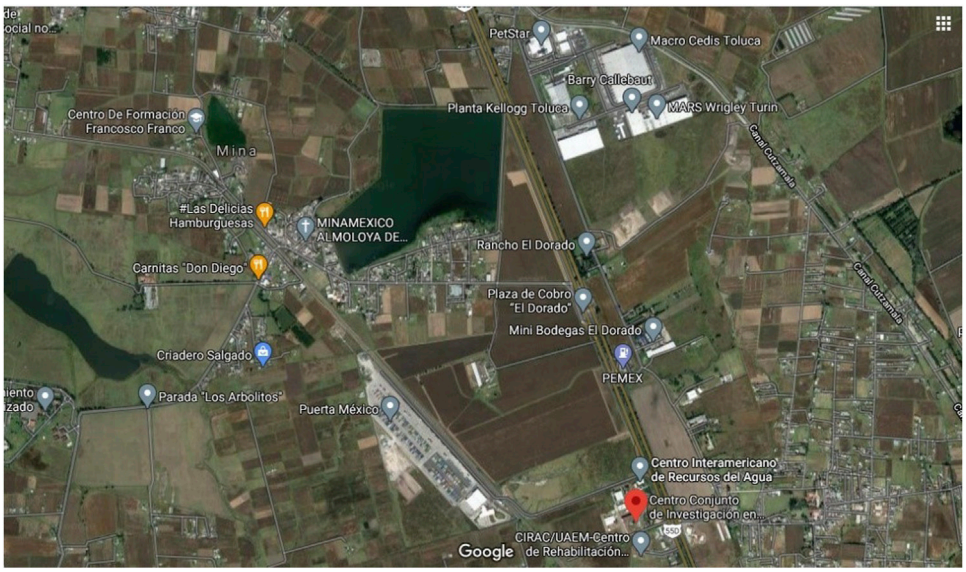

FIGURE 1 | Sampling site of a rural area, located at coordinates 19–40′04.93′N and 99′.71‴56.69′E in Toluca, state of Mexico, Mexico.

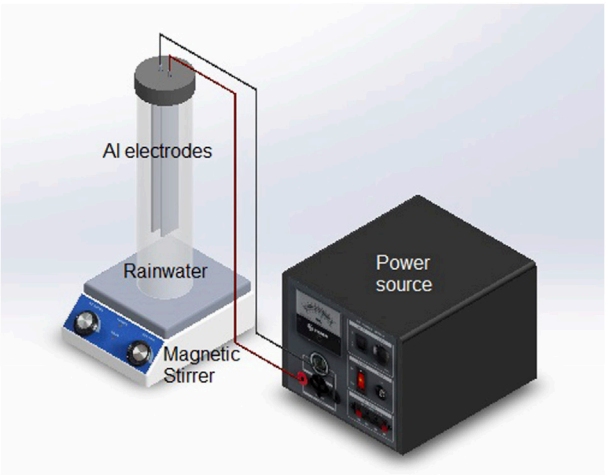

FIGURE 2 | Schematic view of experimental setup.

a rural area. This region is surrounded by agriculture, livestock, and some industrial zones. So, these multiple anthropogenic activities emit different pollutants into the atmosphere, which subsequently precipitate with the rain.

Electrocoagulation Process

The batch EC experiments were conducted with a monopolar cell in a 600 ml glass reactor. The volume treated was 500 ml of rainwater (**Figure 2**), the sample pH was 6.25 ± 0.15, sea salt and sodium sulfate were added as supporting electrolytes at 5×10^{-3} M (0.034 g L^{-1}), and experiments were carried out at 400 rpm and 293 K. The electrochemical cell consists of an aluminum anode and cathode. The dimensions of the Al electrodes were 20 × 2.5 × 0.2 cm, with an anodic area of 50 cm^2, and the distance between the electrodes was 1.0 cm. The current intensity: 0.05—0.15 A (1 and 3 mA/cm^2, of current density, respectively), was supplied with a Steren power source and monitored with a Steren multimeter model UL-28 at different times between 0 and 17 min.

Analysis Methods

The reagents used as supporting electrolyte were food grade sea salt and sodium sulfate Anhydrous Powder (J.T. Baker, Analytical Grade). The samples were characterized before and after treatment, according to the standard methods (American Water Works Association, and Water Environment Federation et al., 2017), pH (pH meter HANNA HI98190), turbidity (HF Scientific® Micro100 Laboratory Turbidimeter), chemical oxygen demand (COD), biochemical oxygen demand (BOD_5), nitrates, and ammoniacal nitrogen (HACH DR5000) and metals, including Mn, Fe, Cu, Zn, Pb, Na, and Al, were determined using Atomic Adsorption (SpectrAA 240 FS spectrophotometer).

The equipment used for the physical chemical analyses were spectrophotometer UV-VIS 1, Model: DR 6000, Brand: HACH, spectrophotometer UV-VIS, Model: Cary 1E, Brand: Varian, conductometer CG/EM, Model: Orion Star A212, turbidimeter Model: micro 100 turbidimeter, Brand: Itfscientific.inc. and potentiometer Model: ION 7000 Brand: OAKTON. Analytical balance: BEL engineering.

Experimental Design

Optimization of the electrochemical process using the RSM has been used due to the possibility of optimizing several parameters simultaneously in order to obtain the experimental design and mathematical modeling (Suárez-Escobar et al., 2016). A CCD was used to evaluate the factors that significantly affect and optimize the operating conditions for the removal of pollutants from rainwater by the EC system. The variables studied are described in **Table 1**.

TABLE 1 | Operational conditions for EC process.

Variable	Value/levels
Contact time	2.93, 5, 10, 15, and 17.07 min
Current density	0.6, 1, 2, 3, and 3.4 mA/cm^2
Support electrolyte	Sea salt and sodium sulfate (0.005M)
Response variables	Turbidity, COD

The proposed experimental design consists of two factors (time and current) and a categorical factor (type of electrolyte A and B), with two blocks of 13 treatments. The experimental design and the statistical analyses were performed using Minitab 19 (Minitab Inc. United States) and the Design Expert® program (Design Expert, Stat-Ease, Inc. United States). As response variables, COD and turbidity were monitored for their availability and viability in the determinations, both to find the best conditions and for comparative purposes with other rainwater treatment methods.

The factors used for the design of experiments were selected according to the literature (Mousazadeh et al., 2021), focusing mainly on current (since the reactions to electrogenerate the coagulant depend on it), the reaction time (because of the amount of coagulant), and the supporting electrolyte (which depends on it too), to determine the effectiveness of the applied current.

RESULTS AND DISCUSSION

Initial Rainwater Characterization

The characterization of the rainwater collected indicated the presence of contaminants such as heavy metals, COD, turbidity, nitrates and ammoniacal nitrogen.

According to the obtained results, the rainwater presented a slightly acidic pH of 6.25, although it is possible that this increase is due to the expected difference between samples. The existence of acid rain is defined by the pH of the rain; thus, the rain that falls on the ground is considered acid rain when its pH is lower than 5.6. The causes of acidity in rain can be from anthropogenic or natural activities. Anthropogenic activities, such as the burning of fossil fuels from transportation or industrial activities, release sulfuric acid and nitric acid into the atmosphere, which are known as inorganic acids. Meanwhile, sources of rain acidity in rural areas come from volatile biogenic organic carbon emissions, such as formic acid, oxalic acid, isoprene, propene, acetic acid, formic acid, or oxalic acid (Payus et al., 2020).

The electrical conductivity is 111 ± 1.5 μS/cm, which shows a low concentration of ions due to the anions, which include 3.82 mg/L NO_3^- and 14 mg/L N-NH_3. Corresponding to the US EPA Report on the Environment from 2014, most airborne NOx originates from combustion-related anthropogenic emissions sources, primarily fossil fuel combustion in electric utilities, high-temperature operations at other industrial sources, and from motor vehicles. It is worth noting the use of home furnaces and gas stoves, which may also produce a considerable quantity of NOx (Keresztesi et al., 2020). Heavy metals were characterized, and 840 μg/L Zn, 130 μg/L Al, 70 μg/L Mn, 32 μg/L Fe, 24 μg/L Cu, and 30 μg/L Pb were found, presenting higher values in contrast with those reported by Rastegari Mehr et al. (2019) This was with the exception of Zn, for which they report higher values (1,320 μg/L Zn) due to several anthropic activities such as vehicular, agricultural and industrial activities, as well as the wind that transports pollutants.

The organic pollutants were also characterized as: 52 mg/L COD, 5.07 mg/L BOD, the poor biodegradability index was 0.097 and a turbidity of 8 NTU. The anthropogenic sources of organics, anions and cations can be from biomass burning, fossil fuel combustion, soil properties and rock weathering, including fertilizers, forest fires and wind-blown dust (Rastegari Mehr et al., 2019; Payus et al., 2020).

Statistical Analysis COD and Turbidity Removal Percentages

Once the electrocoagulation experiments were carried out, the values of the final measurements of COD and Turbidity were acquired after the process. For each sample, the removal of COD and Turbidity was calculated and fitted to a polynomial model to obtain the optimal value of removal percentage for sea salt, as shown in **Figures 3**, **4**.

1) % Removal COD = 113.83—12.22 J—3.23 t + 3.14 J^2 + 0.104 t^2 + 0.426 J^*t
2) % Removal Turbidity = 106.02—5.54 J—1.18 t + 0.27 J^2 + 0.0224 t^2 + 0.231 J^*t

The statistical analyses were presented by response variable (COD and turbidity), and the optimal conditions were obtained simultaneously with the Minitab 19 software. The results of the analysis of variance (ANOVA) are presented in **Table 2** to evaluate the proposed models, which involves the coefficient of determination (R^2), the F value and the *p* value; when the latter are less than 0.05, they indicate that model terms are significant. In this case, electrolyte support, current density, J*E, J^2 and t^2 are significant model terms at the 95% confidence level (Keshtkar et al., 2019).

According to the ANOVA, the correlation coefficient R^2 were 0.97 and 0.55 for the COD removal efficiency and turbidity models, for **Eqs 1**, **2** respectively, which implied that the COD removal efficiency model can establish an adequate correlation between the independent variables and the responses. The equation in terms of actual factors can be used to make predictions about the response for given levels of each factor. On the other hand, for the turbidity removal efficiency model it is not likely to establish an adequate correlation. In addition, the R^2adj values for COD removal efficiency and turbidity were 0.96 and 0.39 respectively, showing that only less than 4% and 61% of the variation could not be described by the models.

Figure 5A represents the response values for COD removal when the variables t (min) and the current density interact, allowing the optimum operating conditions to be established as: 3.26 mA/cm^2 of density current, pH 6.25, treatment time 11.38 min with sea salt, reaching 100% COD removal for the rainwater treatment system. **Figure 3B** contains color contour

TABLE 2 | ANOVA for quadratic model parameters.

Source	COD				Turbidity			
	GL	Sum of squares	F value	*p* Value	GL	Sum of squares	F value	*p* Value
Model	8	10,329.8	68.27	0.000	8	379.957	2.63	0.045
J. Current density	1	834.0	44.09	0.000	1	108.756	6.03	0.025
t. Time	1	2.7	0.14	0.712	1	1.255	0.07	0.795
E. Electrolyte Support	1	9,125.8	482.43	0.000	1	98.826	5.48	0.032
J^2	1	137.6	7.27	0.015	1	1.004	0.06	0.816
t^2	1	94	4.97	0.040	1	4.352	0.24	0.630
J*t	1	36.4	1.92	0.184	1	56.313	3.12	0.095
J*E	1	107.6	5.69	0.029	1	49.963	2.77	0.114
t*E	1	18.0	0.95	0.343	1	59.942	3.32	0.086
Error	17	321.6			17	306.776		
Lack of fit	9	261.7	3.89	0.035	9	210.919	1.96	0.176
Pure Error	8	59.9			8	95.858		
Total	25	10,651.4			25	686.733		
	R^2	0.9698			R^2	0.5533		
	R^2adj	0.9556			R^2adj	0.3431		

bands representing ranges of the fitted response values. The highest values of COD removal for rainwater are found on the right side of the graph, which coincides with the high values of mean current density and the relationship with contact time. The lowest COD removal values for rainwater are found on the left side of the graph, which coincides with the low values for current density. **Figure 3C** shows the Pareto graph, which confirms what was obtained in the ANOVA, where it is observed that the current density, the supporting electrolyte, the quadratic term of the current density and the interaction between the current density and the supporting electrolyte have a significant effect on the removal efficiency of the COD.

Figure 4A represents the response values of the turbidity removal when the variables t (min) and current density interact, which allows establishing the optimal operating conditions for the rainwater treatment system. **Figure 6B** contains contour bands representing ranges of the adjusted response values. The highest turbidity removal values for rainwater are found on the left side of the graph, which coincides with the highest values of current density and the relationship with contact time. The lowest turbidity removal values for rainwater are found on the left side of the graph, which matches with the highest values of current density and the relationship with the lowest value of contact time. **Figure 6C** shows the Pareto graph, where it is observed that the current density and the supporting electrolyte have a significant effect on the Turbidity removal efficiency.

Electrolysis Time

Electrolysis time is an underlying factor leading to a significant difference in the removal efficiency. **Figure 3** illustrates the removal efficiency of COD_0 = 52 mg/L at pH 6.55–7.89, with treatment time from 0 to 16 min at 3 mA/cm^2. The removal efficiency reached approximately 99.9% at 10 min, with a 25 mg/L Al dose. According to the kinetics, at 11 min the complete removal of COD was achieved, so no additional time is required. The produced amount of metal ions was calculated by Faraday's Law equation (**Eq. 1**):

$$m = \frac{ItM}{FZ} \tag{1}$$

where M and Z in **Eq. 1** represent Al molar mass (g/mol), and oxidation state in solution, respectively, and *I* the current (A). F is the Faraday's constant equal to 96,485 C/mol. The amount of aluminum produced is $m = 12.5\,mg$ Al, the total volume is 0.5 L, then 25 mg/L Al was the optimal dose (72 mg/L $Al(OH)_3$). Additionally, a study carried out for the treatment of wastewater with the generation of 0.17 g of Al to treat 500 ml of wastewater for 15 min and with 0.04 A is reported (Molano-Mendoza et al., 2018; Padmaja et al., 2020).

In addition, **Figure 3** shows the kinetic COD, kinetic constants and the correlation coefficients fitted to the second order model k = 0.4828 L/mg min^{-1} and R^2 = 0.9925

$$C = \frac{dC}{dt} = k_2 t^2 \tag{2}$$

Initial pH Effect

According to the species distribution diagram performed *via* medusa program (**Supplementary Figure S1**), the predominant species in the pH range monitored during treatment (6.25–7.89) is $Al(OH)_3$ which promotes coagulation-flocculation of colloidal particles present in rainwater, promoting the removal of COD, turbidity and some metals.

Eqs 3–5 show the electrochemical reactions and solution reactions carried out in the batch EC process that involve the oxidation of Al to Al^{3+}. The H_2O reduction to H_2 and OH^- ions is carried out on the cathode. The solution reactions show the formation of metallic hydroxides. Because aluminum hydroxide is an amphoteric hydroxide, the pH is a vulnerable factor for the formation of $Al(OH)_3$ (**Eq. 5**) flocs. The solubility of aluminum is in balance with the solid phase $Al(OH)_3$ depending upon the surrounding pH, since solid $Al(OH)_3$ is more common among pH 4.5 and 12, and higher pH 10, the soluble species $Al(OH)_4^-$ is

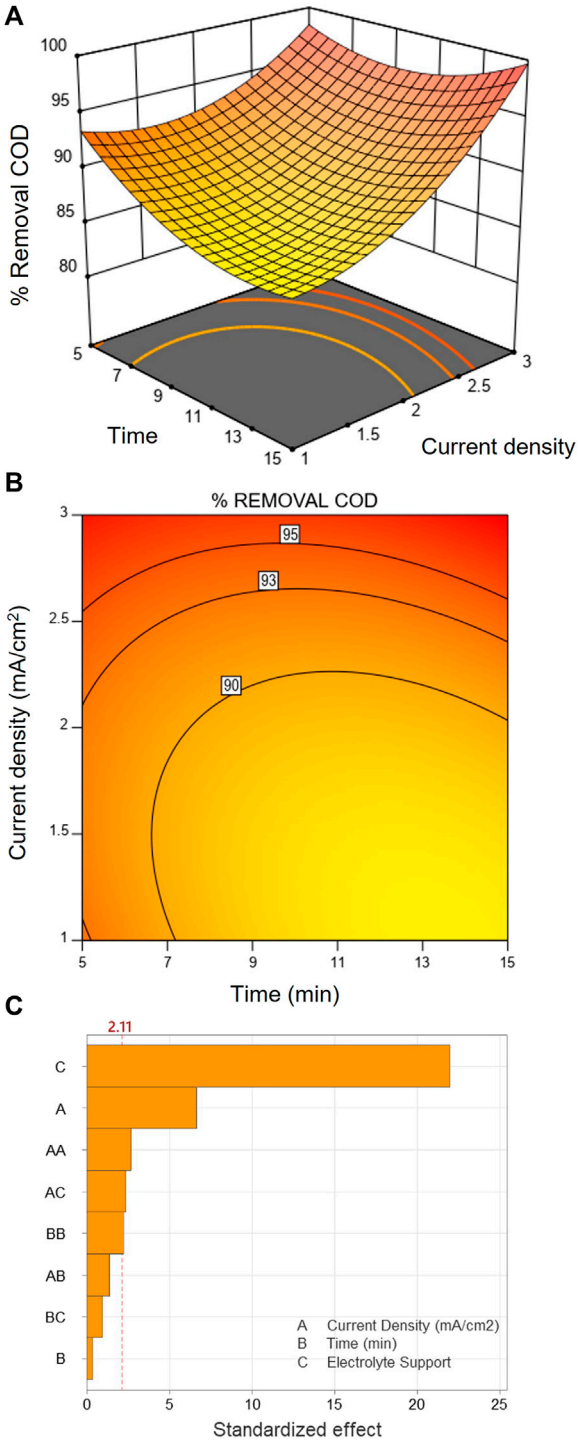

FIGURE 3 | (A) 3D Response Surface of the effect of current density (mA/cm^2), time (min) and electrolyte support (sea salt 0.005 M). **(B)** Contour plot of t (min) versus density (mA/cm^2). **(C)** Pareto plots of standardized effects, all on the COD removal efficiency.

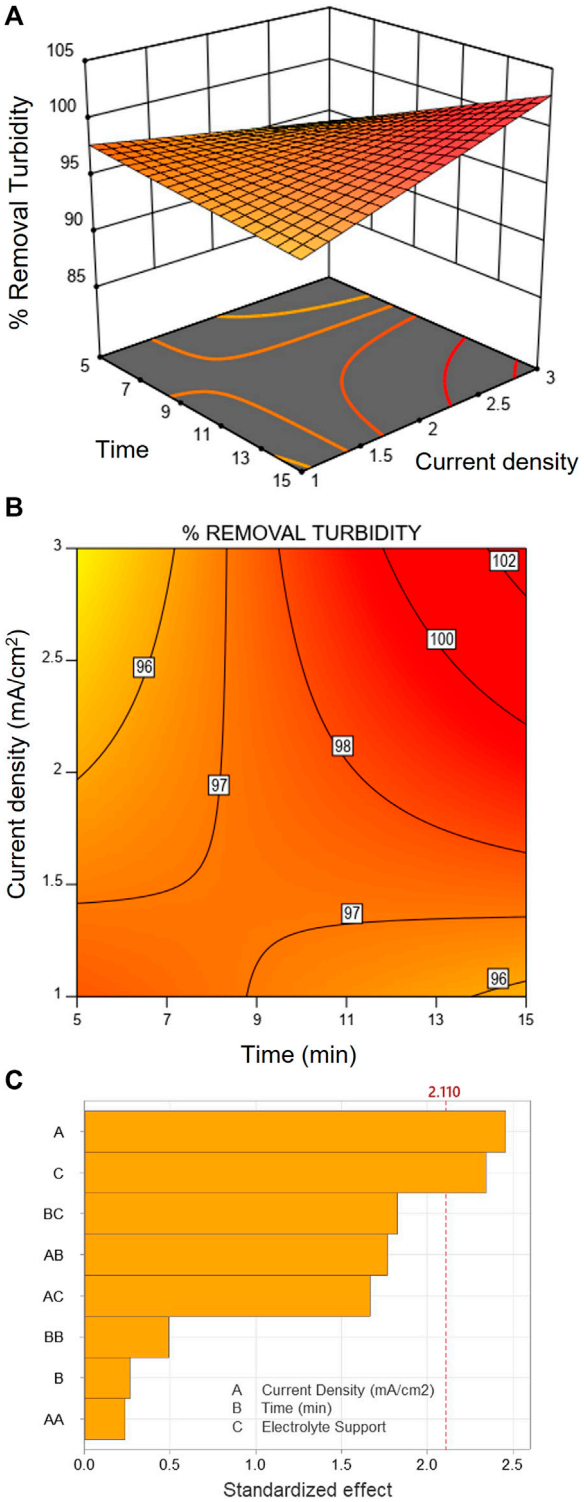

FIGURE 4 | (A) 3D Response Surface of the effect of current density (mA/cm^2), time (min) and electrolyte support (sea salt 0.005 M). **(B)** Contour plot of t (min) versus density (mA/cm^2). **(C)** Pareto plots of standardized effects, all on the turbidity removal efficiency.

TABLE 3 | Experimental design: response surface methodology (RSM) central composite design (CCD) for COD and turbidity removal efficiency.

Run	Real values		% Removal			
			Sea salt		Sodium sulfate	
	Current density (mA/cm^2)	Time (min)	COD	Turbidity	COD	Turbidity
1	0.58	10.00	83.93	99.97	40.28	93.67
2	1.00	5.00	100.00	99.98	48.61	93.93
3	1.00	15.00	85.71	99.98	52.78	76.60
4	2.00	2.93	87.50	99.95	59.72	99.07
5	2.00	10.00	91.07	99.99	48.61	83.13
6	2.00	10.00	91.07	99.99	50	93.93
7	2.00	10.00	85.71	99.99	47.22	94.53
8	2.00	10.00	89.29	99.99	48.61	93.93
9	2.00	10.00	94.64	99.99	52.78	93.60
10	2.00	17.07	89.29	100.00	55.56	98.60
11	3.00	5.00	100.00	99.97	63.89	99
12	3.00	15.00	100.00	100.00	70.83	99.27
13	3.40	10.00	100.00	99.99	72.22	98.80

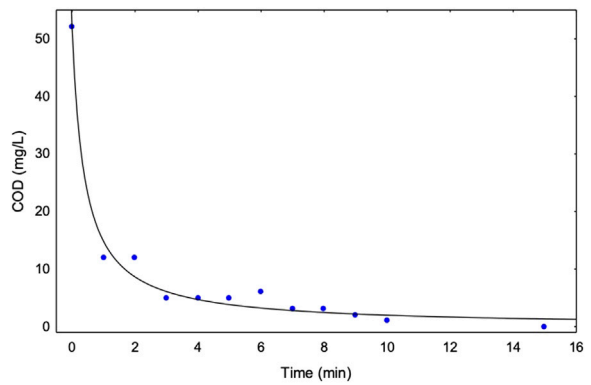

FIGURE 5 | Removal of COD (mg/L) for rainwater electrocoagulation process. COD_0 = 52 mg/L at initial pH 6.55, treatment time 15 min, at 0.15A and 72 mg/L $Al(OH)_3$ dose.

the prevalent species, as shown in the species distribution diagram (**Eq. 6**).

Anodic reactions:

$$Al \rightarrow Al^{3+} + 3e^{-} \tag{3}$$

Cathodic reaction:

$$2H_2O + 2e^{-} \rightarrow H_2 \uparrow + 2OH^{-} \tag{4}$$

Solution reactions:

$$Al^{3+} + 6H_2O \rightarrow Al(OH)_{3(s)} \downarrow + 3H_3O^{+} \tag{5}$$

$$Al(OH)_{3(s)} + OH^{-} \rightarrow Al(OH)_4^{-} \tag{6}$$

During the electrogeneration of the coagulant ($Al(OH)_3$ (**Eq. 5**), small flocs are formed where both the colloidal organic matter and the metallic ions of the rainwater are adsorbed. The

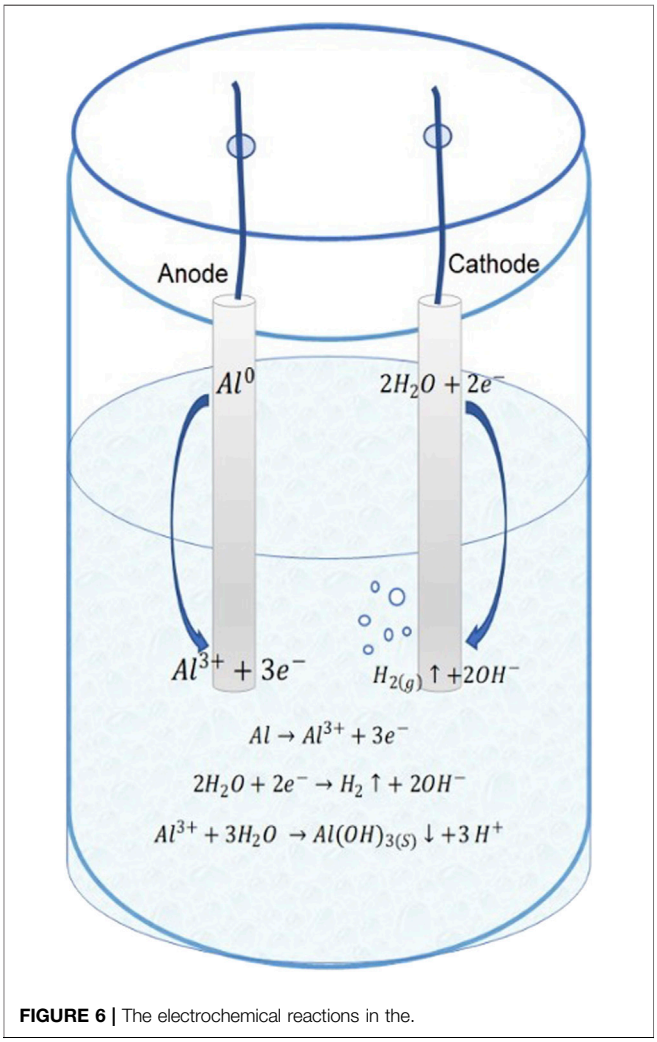

FIGURE 6 | The electrochemical reactions in the.

TABLE 4 | Physicochemical characterization: before and after electrochemical treatment. Mexican and international laws for drinking water.

Parameter	Initial sample	Final sample	Mexican lows	International lows	
			NOM-127-SSA1-1994	US EPA	European commission drinking water directive (98/83/EC)
EC (μS/cm)	111 ± 1.5	256 ± 0.10	—	—	2.5 (20°C)
pH	6.25 ± 1.5	8.26 ± 0.5	6.5–8.5	6.5–8.5	6.5–9.5
Turbidity (NTU)	8.00 ± 0.31	0.08 ± 0.32	5>	—	AC
COD (mg/L)	52	0	—	—	—
BOD_5 (mg/L)	5.07	—	—	—	—
$N\text{-}NH_3$ (mg/L)	14 ± 1	0	0.50	—	—
NO_3^- (mg/L)	3.82	1.1	0.05	—	—
Na (mg/L)	0.06	17.52	200	—	200
Al (mg/L)	130 μg/L	N/D	0.20	0.5–0.2	0.20
Mn (mg/L)	70 μg/L	11 μg/L	0.15	0.05	0.05
Fe (mg/L)	32 μg/L	25 μg/L	0.30	0.30	0.20
Cu (mg/L)	24 μg/L	35 μg/L	2.00	1	2
Zn (mg/L)	840 μg/L	17 μg/L	5.00	5	—
Pb (mg/L)	30 μg/L	16 μg/L	0.01	0	0.10

AC: acceptable to the consumer and without abnormal change.

TABLE 5 | Costs and energy consumption of electrochemical treatments with different types of water.

Types of water	Electrode system/reactor, j, mA/cm^2	Costs USD/m^3/energy consumption kWh/m^3	References
chocolate industry wastewater	Downflow column aluminium electrodes	4.01/94.79	García-Orozco et al. (2021)
slaughterhouse wastewater	steel or aluminum electrodes, bipolar (BP) or monopolar configuration system	4.19 ± 0.12 kW h/m^3	Asselin et al. (2008)
sugar industry wastewater	iron as electrode	5.25/42	Sahu & Chaudhari, (2015)
dairy industry wastewater	electrode of iron containing six plates	1.04/4.5	Geraldino et al. (2015)
Rain water	aluminum electrodes	0.014/0.18	This study

generation of H_2 bubbles in the cathode due to the reduction of water (**Eq. 4**) benefits the separation of the light flocs by the electroflotation process. Additionally, the bubbles contribute to the hydrodynamics of the reactor through convection, favoring quick contact among the species so that with the treatment time, the flocs increase in size, generating the coagulation process, and finally precipitation occurs (see **Figure 6**) (Mousazadeh et al., 2021; Shakeri et al., 2021).

Effect of Current Density

The experiments were carried out with a combination of Al/Al electrodes in an electrolysis time range of 2.93–17 min. The effect of current (0.58–3.40 mA/cm^2) was evaluated on COD and turbidity according to the experimental design (**Table 3**). From the results obtained, **Figures 5**, **6** show that the removal efficiency increases with the increase in current density with a time of 15 min, reaching 100% removal for COD and turbidity with 3.26 mA/cm2 of current and 11.26 min (Padmaja et al., 2020). The increase in removal efficiency with the higher current (3 mA/cm^2) is due to the greater amount of coagulant resulting in more active sites for COD removal. Likewise, more oxidation of the anode is generated and, therefore, more Al ions according to Faraday's law. In addition, as more Al is produced, it reacts with more OH^- ions to create aluminum hydroxide, which acts as an adsorbent that can adsorb/remove contaminants (Negarestani et al., 2020). In this study, the COD content decreased from 52 to 0 mg/L, showing to be more efficient compared to what was reported by Xu et al. (2021), who reported a decrease of 1.7 to 1.0 mg/L of COD through electrocoagulation coupled with a gravity-driven membrane for rainwater treatment (Du et al., 2019; Xu et al., 2021).

Effect of Supporting Electrolyte

One of the most important parameters for the proper functioning of electrochemical cells is the supporting electrolyte, which ensures that the ionic conductivity is sufficient, and the applied current is used to the maximum (Maitlo et al., 2018).

According to the data in **Table 3**, the composite sample of rainwater represents 100% removal for turbidity and COD parameters using sea salt as the electrolyte, and 70.83% for COD and 99.27% for turbidity with sodium sulfate under the same conditions of treatment time (15 min) and density of applied current (3 mA/cm^2) in both cases.

In this particular case, the two electrolytes used were 0.05 M Na_2SO_4 with a conductivity of 237 μS/cm, and for sea salt, the amount equivalent to that of sodium sulfate was added,

registering a conductivity of 305 μS/cm; the ionic conductivity increases because in the composition of the sea salt there is 86% NaCl, so conductivity is improved and therefore the applied current is used properly during the treatment. This gives rise to reactions 3 and 4 for the electrogeneration of the coagulant with greater efficiency, thus achieving in a short time total elimination of COD and turbidity. Sea salt provides some additional benefits, like stabilizing the electrochemical process, whilst also providing other essential minerals such as Na, Cl, Mg, S, Ca, Br, and K for human use and consumption.

The Cl^-contents are another advantage of electrocoagulation using sea salt, as the electrogeneration of Cl_2 (**Eq. 7**) is carried out at the anode, and subsequently $ClO^-$is produced, which act as disinfectant (Yildiz et al., 2008; Jaiyeola, 2017).

$$2\,Cl^- \rightarrow Cl_2 + 2e^- \quad (7)$$

$$Cl_2 + H_2O \rightarrow ClO^- + H^+ + Cl^- \quad (8)$$

Therefore, the generation of Cl_2 can act in two ways: 1) it can directly oxidize organic matter (including the cell wall of bacteria) and 2) Cl_2 with water generates ClO^-which can continue to oxidize organic matter, that at the same time is adsorbed in the generated coagulant and is finally separated by flotation or sedimentation. Thus, it can be suggested that a disinfection was carried out (Aguilar-Ascon, 2019), since both parameters can be related to the elimination of possible microorganisms found in the suspended particles that generate turbidity and at the same time provide organic matter. Furthermore, it has been reported that rainwater contains a wide variety of microorganisms (Yildiz et al., 2008; Jaiyeola, 2017).

Some studies show different treatments and removal efficiencies for rainwater; Aljerf (2018) reported a modern PVC-filter filled with reused glass and crushed foam glass for the removal of major contaminants in rainwater to improve the physical properties and enhance the matrix of this potential source of water with important minerals. The turbidity parameter was 8.3 NTU, and total removal of COD after treatment was achieved. Heavy metals were also decreased: Al (100%), Mn (84.3%), Zn (98%), Fe (21.9%), and Pb (46.7%). Leong et al., 2018, reported the following removal data for the treatment of rainwater: COD (56% of 71 mg/L), turbidity (38% of 3.8 NTU), Cu (63%) and Zn (62% of 0.013 mg/L).

Final Characterization

Table 4 shows the final characterization of rainwater before and after EC treatment, under optimal pH conditions set to 6.25, treatment time 11.38 min at 3.26 mA/cm^2 with 25 mg/L Al dose. The electrical conductivity was increased due to supporting electrolyte addition, from 115.16 to 256 μS/cm (+130.32%), mainly Na^+ (from 0.06 to 17.52 mg/L). This value improves the physical-chemistry quality of rainwater according to the European Community. Final pH was increased at 8.26 ± 0.5. Turbidity was reduced from 8.0 to 0.08 (99.99%). COD, BOD, N-NH_3 were 100% removed. Metals were reduced significantly: Al (100%), Mn (84.29%), Fe (21.87%). Cu was slightly increased from 24 to 35 μg/L (48.5%), although this value is under the permissible limit. Zn was reduced from 840 to 17 μg/L (97.97%), Pb from 30 to 16 μg/L (46.6%).

Energy Consumption

For EC process the electrical energy costs were estimated as shown in **Eq. 9**:

$$C_{energy}\left(\frac{kWh}{m3}\right) = \frac{U\,x\,I\,x\,t_{EC}}{1000 * V} \quad (9)$$

where U is the cell voltage (2.4 V), I is the current (0.15 A), t_{EC} is the time of electrolysis (0.25 h) and V is the volume (0.0005 m^3). With these values, energy consumption was 0.18 kWh/m^3 (Taeyeon Kim et al., 2020) for EC treatment and the monetary energy production rate in Mexico is US $ 0.08 for industrial use per kWh, the energy cost is $ 0.014/m^3.

Therefore, the treatment costs are accessible for the implementation of rainwater treatment, compared with other conventional methods such as aerated lagoons, where it is required to apply energy to air generators. Subsequently, it requires a disinfection process, with the produced sludge increasing costs (Mcnaughton et al., 2011). Rainwater filtration is an efficient treatment; however, it also requires disinfection.

It is important to mention that in the literature consulted, no information was found on EC treatments with rainwater, therefore there is no point of comparison regarding costs. However, there are publications that indicate the costs of treating wastewater from various source with EC are varied, as shown in the **Table 5**.

The energy consumption and costs calculated in this study were lower than reported in other studies, although they used to treat different types of wastewater, where costs are between 1.04 and 5.25 USD/m^3 and energy consumption ranges from 4.5 to 95 kWh/m^3 (Asselin et al., 2008; Geraldino et al., 2015; Sahu & Chaudhari, 2015; García-Orozco et al., 2021).

CONCLUSION

The research was carried out on the electrocoagulation treatment with aluminum electrodes in rainwater using the response surface methodology. The optimal operating conditions obtained were: current density 3.26 mA/cm^2, treatment time 11.38 min, with a dose of 25 mg/L Al [72 mg/L $Al(OH)_3$], achieving a removal 100% turbidity, COD, BOD_5, and N-NH_3. Also, metals were significantly reduced.

Another of the factors considered were the electrolyte, for which two support electrolytes were used: 1) sea salt and 2) sodium sulfate, showing that sea salt gives better results for the removal of COD, turbidity and physicochemical quality.

The main advantages of the electrocoagulation treatment were a short treatment time (15 min), significant removal of organic and inorganic physicochemical parameters,

complying with the parameters established by the EPA and the European Community, low cost, it is a post-treatment rainwater free of residual aluminum and minimal generation of sludge as waste compared to other treatments reported in the literature. The main benefit is that the support electrolyte is food grade, so rainwater can be used for human consumption.

In addition, being an integral electrocoagulation process, it has the advantage of removing organic and inorganic matter, along with additional disinfection, producing a controlled amount of sludge (Mcnaughton et al., 2011). Also, to its ease of operation, this process is a viable alternative to be applied in homes that already have a rainwater collection and storage system and adapt it for human consumption.

DATA AVAILABILITY STATEMENT

The datasets presented in this study can be found in online repositories. The names of the repository/repositories and accession number(s) can be found below: http://hdl.handle.net/20.500.11799/110089.

AUTHOR CONTRIBUTIONS

AM-F performed most of the experimental work as well as the literature search, analyses and interpretation of results. IL-H and VM-M supervised the development of the project and contributed to the literature search, analysis and performed most of the interpretation of results of initial and final characterization. GR-M was the project leader and supervisor of the entire development, analyses and interpretation and homogenization of the results and their presentation. ET-S performed most of the multivariate analysis and the kinetic removal model, supervised part of the experimental work and contributed to the literature search, analysis and interpretation of results, as well as to homogenizing results and their presentation. AG-M supervised part of the experimental work. All authors have read and agreed with the published version of the manuscript.

ACKNOWLEDGMENTS

The authors thank the Interamerican Institute of Water Technology and Sciences, Autonomous University of the State of Mexico for the financial support granted through the Project number 6449/2022CIB, 0549292 UAEMex research project and the National Council of Science and Technology (CONACYT) for the studentship (No 930437) for Alejandra Morales Figueroa.

SUPPLEMENTARY MATERIAL

The Supplementary Material for this article can be found online at: https://www.frontiersin.org/articles/10.3389/fenvs.2022.860011/full#supplementary-material

REFERENCES

Adachi, K., and Buseck, P. R. (2015). Changes in Shape and Composition of Sea-Salt Particles upon Aging in an Urban Atmosphere. *Atmos. Environ.* 100, 1–9. doi:10.1016/j.atmosenv.2014.10.036

Aguilar-Ascon, E. (2019). Removal of Escherichia coli from Domestic Wastewater Using Electrocoagulation. *J. Ecol. Eng.* 20 (5), 42–51. doi:10.12911/22998993/105331

Aljerf, L. (2018). Advanced Highly Polluted Rainwater Treatment Process. *Juee* 12 (1), 50–58. doi:10.4090/juee.2018.v12n1.050058

American Water Works Association and Water Environment Federation (2017). "STANDARD METHODS FOR THE EXAMINATION OF WATER AND WASTEWATER," in *American Public Health Association*. Editors Andrew D. Eaton, A. E. G., and Clesceri, L. S. 23rd Edn (United States: American Water Works Association, and Water Environment Federation).

Asselin, M., Drogui, P., Benmoussa, H., and Blais, J.-F. (2008). Effectiveness of Electrocoagulation Process in Removing Organic Compounds from Slaughterhouse Wastewater Using Monopolar and Bipolar Electrolytic Cells. *Chemosphere* 72 (11), 1727–1733. doi:10.1016/j.chemosphere.2008.04.067

Darvishmotevalli, M., Zarei, A., Moradnia, M., Noorisepehr, M., and Mohammadi, H. (2019). Optimization of Saline Wastewater Treatment Using Electrochemical Oxidation Process: Prediction by RSM Method. *MethodsX* 6, 1101–1113. doi:10.1016/j.mex.2019.03.015

Devlin, T. R., Kowalski, M. S., Pagaduan, E., Zhang, X., Wei, V., and Oleszkiewicz, J. A. (2019). Electrocoagulation of Wastewater Using Aluminum, Iron, and Magnesium Electrodes. *J. Hazard. Mater.* 368, 862–868. doi:10.1016/j.jhazmat.2018.10.017

Ding, A., Wang, J., Lin, D., Cheng, X., Wang, H., Bai, L., et al. (2018). Effect of PAC Particle Layer on the Performance of Gravity-Driven Membrane Filtration (GDM) System during Rainwater Treatment. *Environ. Sci. Water Res. Technol.* 4 (1), 48–57. doi:10.1039/c7ew00298j

Ding, A., Wang, J., Lin, D., Tang, X., Cheng, X., Wang, H., et al. (2017). A Low Pressure Gravity-Driven Membrane Filtration (GDM) System for Rainwater Recycling: Flux Stabilization and Removal Performance. *Chemosphere* 172, 21–28. doi:10.1016/j.chemosphere.2016.12.111

Du, X., Xu, J., Mo, Z., Luo, Y., Su, J., Nie, J., et al. (2019). The Performance of Gravity-Driven Membrane (GDM) Filtration for Roofing Rainwater Reuse: Implications of Roofing Rainwater Energy and Rainwater Purification. *Sci. Total Environ.* 697, 134187. doi:10.1016/j.scitotenv.2019.134187

Dura, A., and Breslin, C. B. (2019). Electrocoagulation Using Aluminium Anodes Activated with Mg, in and Zn Alloying Elements. *J. Hazard. Mater.* 366, 39–45. doi:10.1016/j.jhazmat.2018.11.094

García-Orozco, V. M., Roa-Morales, G., Linares-Hernández, I., Serrano-Jimenes, I. J., Salgado-Catarino, M. A., and Natividad, R. (2021). Electrocoagulation of a Chocolate Industry Wastewater in a Downflow Column Electrochemical Reactor. *J. Water Process Eng.* 42, 102057. doi:10.1016/j.jwpe.2021.102057

Geraldino, H. C. L., Simionato, J. I., Freitas, T. K. F. d. S., Garcia, J. C., Carvalho Júnior, O. D., and Correr, C. J. (2015). Efficiency and Operating Cost of Electrocoagulation System Applied to the Treatment of Dairy Industry Wastewater. *Acta Sci. Technol.* 37 (3), 401–408. doi:10.4025/actascitechnol.v37i3.26452

Izquierdo, C. J., Canizares, P., Rodrigo, M. A., Leclerc, J. P., Valentin, G., and Lapicque, F. (2010). Effect of the Nature of the Supporting Electrolyte on the Treatment of Soluble Oils by Electrocoagulation. *Desalination* 255 (1–3), 15–20. doi:10.1016/j.desal.2010.01.022

Jaiyeola, A. T. (2017). The Management and Treatment of Airport Rainwater in a Water-Scarce Environment. *Int. J. Environ. Sci. Technol.* 14 (2), 421–434. doi:10.1007/s13762-016-1122-0

Keresztesi, Á., Nita, I.-A., Boga, R., Birsan, M.-V., Bodor, Z., and Szép, R. (2020). Spatial and Long-Term Analysis of Rainwater Chemistry over the Conterminous United States. *Environ. Res.* 188, 109872. doi:10.1016/j.envres.2020.109872

Keshtkar, A. R., Moosavian, M. A., Sohbatzadeh, H., and Mofras, M. (2019). La(III) and Ce(III) Biosorption on Sulfur Functionalized Marine Brown Algae Cystoseira Indica by Xanthation Method: Response Surface Methodology, Isotherm and Kinetic Study. *Groundw. Sustain. Dev.* 8, 144–155. doi:10.1016/j.gsd.2018.10.005

Keyikoglu, R., Can, O. T., Aygun, A., and Tek, A. (2019). Comparison of the Effects of Various Supporting Electrolytes on the Treatment of a Dye Solution by Electrocoagulation Process. *Colloid Interface Sci. Commun.* 33, 100210. doi:10.1016/j.colcom.2019.100210

Khayan, K., Heru Husodo, A., Astuti, I., Sudarmadji, S., and Sugandawaty Djohan, T. (2019). Rainwater as a Source of Drinking Water: Health Impacts and Rainwater Treatment. *J. Environ. Public Health* 2019, 1–10. doi:10.1155/2019/1760950

Kim, T., Kim, T.-K., and Zoh, K.-D. (2020). Removal Mechanism of Heavy Metal (Cu, Ni, Zn, and Cr) in the Presence of Cyanide during Electrocoagulation Using Fe and Al Electrodes. *J. Water Process Eng.* 33, 101109. doi:10.1016/j.jwpe.2019.101109

Kim, T., Lye, D., Donohue, M., Mistry, J. H., Pfaller, S., Vesper, S., et al. (2016). Harvested Rainwater Quality before and after Treatment and Distribution in Residential Systems. *J. Am. Water Works Assoc.* 108 (11), E571–E584. doi:10.5942/jawwa.2016.108.0182

Leong, J. Y. C., Chong, M. N., and Poh, P. E. (2018). Assessment of Greywater Quality and Performance of a Pilot-Scale Decentralised Hybrid Rainwater-Greywater System. *J. Clean. Prod.* 172, 81–91. doi:10.1016/j.jclepro.2017.10.172

Leong, J. Y. C., Oh, K. S., Poh, P. E., and Chong, M. N. (2017). Prospects of Hybrid Rainwater-Greywater Decentralised System for Water Recycling and Reuse: A Review. *J. Clean. Prod.* 142, 3014–3027. doi:10.1016/j.jclepro.2016.10.167

Maitlo, H. A., Kim, J. H., An, B. M., and Park, J. Y. (2018). Effects of Supporting Electrolytes in Treatment of Arsenate-Containing Wastewater with Power Generation by Aluminumair Fuel Cell Electrocoagulation. *J. Industrial Eng. Chem.* 57, 254–262. doi:10.1016/j.jiec.2017.08.031

Mcnaughton, E., Stoll, S. J., Smith, J. E. J., Middlebrooks, E. J., and Bowman, R. H. (2011). *Principles of Design and OperationsP Rinciples of Design and Operations of Wastewater Treatment Pond Systems O F Wastewater Treatment Pond Systems for Plant Operators, Engineers, and Managers*. Washington, D.C., United States: U.S. Environmental Protection Agency, 457. EPA/600/R-.

Molano-Mendoza, M., Donneys-Victoria, D., Marriaga-Cabrales, N., Mueses, M. A., Li Puma, G., and Machuca-Martínez, F. (2018). Synthesis of Mg-Al Layered Double Hydroxides by Electrocoagulation. *MethodsX* 5, 915–923. doi:10.1016/j.mex.2018.07.019

Mousazadeh, M., Naghdali, Z., Al-Qodah, Z., Alizadeh, S. M., Karamati Niaragh, E., Malekmohammadi, S., et al. (2021). A Systematic Diagnosis of State of the Art in the Use of Electrocoagulation as a Sustainable Technology for Pollutant Treatment: An Updated Review. *Sustain. Energy Technol. Assessments* 47, 101353. doi:10.1016/j.seta.2021.101353

Omar, K. F. M., Aziz, N. A. A., Palaniandy, P., and Abu Amr, S. S. (2017). Removal of Lindane and Escherichia coli (E.Coli) from Rainwater Using Photocatalytic and Adsorption Treatment Processes. *Glob. Nest J.* 19 (2), 191–198. doi:10.30955/gnj.002061

Padmaja, K., Cherukuri, J., and Anji Reddy, M. (2020). A Comparative Study of the Efficiency of Chemical Coagulation and Electrocoagulation Methods in the Treatment of Pharmaceutical Effluent. *J. Water Process Eng.* 34, 101153. doi:10.1016/j.jwpe.2020.101153

Payus, C. M., Jikilim, C., and Sentian, J. (2020). Rainwater Chemistry of Acid Precipitation Occurrences Due to Long-Range Transboundary Haze Pollution and Prolonged Drought Events during Southwest Monsoon Season: Climate Change Driven. *Heliyon* 6 (9), e04997. doi:10.1016/j.heliyon.2020.e04997

Rastegari Mehr, M., Keshavarzi, B., and Sorooshian, A. (2019). Influence of Natural and Urban Emissions on Rainwater Chemistry at a Southwestern Iran Coastal Site. *Sci. Total Environ.* 668, 1213–1221. doi:10.1016/j.scitotenv.2019.03.082

Sahu, O. P., and Chaudhari, P. K. (2015). Electrochemical Treatment of Sugar Industry Wastewater: COD and Color Removal. *J. Electroanal. Chem.* 739, 122–129. doi:10.1016/j.jelechem.2014.11.037

Shakeri, E., Mousazadeh, M., Ahmadpari, H., Kabdasli, I., Jamali, H. A., Graça, N. S., et al. (2021). Electrocoagulation-flotation Treatment Followed by Sedimentation of Carpet Cleaning Wastewater: Optimization of Key Operating Parameters via RSM-CCD. *Desalination Water Treat.* 227, 163–176. doi:10.5004/dwt.2021.27307

Suárez-Escobar, A., Pataquiva-Mateus, A., and López-Vasquez, A. (2016). Electrocoagulation-photocatalytic Process for the Treatment of Lithographic Wastewater. Optimization Using Response Surface Methodology (RSM) and Kinetic Study. *Catal. Today* 266, 120–125. doi:10.1016/j.cattod.2015.09.016

Taffere, G. R., Beyene, A., Vuai, S. A. H., Gasana, J., and Seleshi, Y. (2017). Dilemma of Roof Rainwater Quality: Applications of Physical and Organic Treatment Methods in a Water Scarce Region of Mekelle, Ethiopia. *Urban Water J.* 14 (5), 460–466. doi:10.1080/1573062X.2016.1176225

Teixeira, C. A., and Ghisi, E. (2019). Comparative Analysis of Granular and Membrane Filters for Rainwater Treatment. *Water* 11 (5), 1004. doi:10.3390/w11051004

Verma, A. K. (2017). Treatment of Textile Wastewaters by Electrocoagulation Employing Fe-Al Composite Electrode. *J. Water Process Eng.* 20, 168–172. doi:10.1016/j.jwpe.2017.11.001

Waso, M., Khan, S., Singh, A., McMichael, S., Ahmed, W., Fernández-Ibáñez, P., et al. (2020). Predatory Bacteria in Combination with Solar Disinfection and Solar Photocatalysis for the Treatment of Rainwater. *Water Res.* 169, 115281. doi:10.1016/j.watres.2019.115281

Xu, J., Du, X., Zhao, W., Wang, Z., Lu, X., Zhu, L., et al. (2021). Roofing Rainwater Cleaner Production Using Pilot-Scale Electrocoagulation Coupled with a Gravity-Driven Membrane Bioreactor (EC-GDMBR): Water Treatment and Energy Efficiency. *J. Clean. Prod.* 314, 128055. doi:10.1016/j.jclepro.2021.128055

Yıldız, Y. Ş., Koparal, A. S., and Keskinler, B. (2008). Effect of Initial pH and Supporting Electrolyte on the Treatment of Water Containing High Concentration of Humic Substances by Electrocoagulation. *Chem. Eng. J.* 138 (1–3), 63–72. doi:10.1016/j.cej.2007.05.029

Zhang, K., Randelovic, A., Page, D., McCarthy, D. T., and Deletic, A. (2014). The Validation of Stormwater Biofilters for Micropollutant Removal Using *In Situ* Challenge Tests. *Ecol. Eng.* 67, 1–10. doi:10.1016/j.ecoleng.2014.03.004

Conflict of Interest: The authors declare that the research was conducted in the absence of any commercial or financial relationships that could be construed as a potential conflict of interest.

Publisher's Note: All claims expressed in this article are solely those of the authors and do not necessarily represent those of their affiliated organizations, or those of the publisher, the editors and the reviewers. Any product that may be evaluated in this article, or claim that may be made by its manufacturer, is not guaranteed or endorsed by the publisher.